Experimental evidence of inertial dynamics in ferromagnets

Kumar Neeraj[1,†], Nilesh Awari[2,†], Sergey Kovalev[2], Debanjan Polley[1], Nanna Zhou Hagström[1], Sri Sai Phani Kanth Arekapudi[3], Anna Semisalova[4,5], Kilian Lenz[5], Bertram Green[2], Jan-Christoph Deinert[2], Igor Ilyakov[2], Min Chen[2], Mohammed Bawatna[2], Valentino Scalera[6], Massimiliano d'Aquino[7], Claudio Serpico[6], Olav Hellwig[3,5], Jean-Eric Wegrowe[8], Michael Gensch[9,10], and Stefano Bonetti [*1,11]

[1]Department of Physics, Stockholm University, 106 91 Stockholm, Sweden
[2]Institute of Radiation Physics, Helmholtz-Zentrum Dresden-Rossendorf, 01328 Dresden, Germany
[3]Institute of Physics, Chemnitz University of Technology, 09107 Chemnitz, Germany
[4]Faculty of Physics, University of Duisburg-Essen, 47057 Duisburg, Germany
[5]Institute of Ion Beam Physics and Materials Research, Helmholtz-Zentrum Dresden-Rossendorf, 01328 Dresden, Germany
[6]DIETI, University of Naples Federico II, Naples, Italy
[7]Department of Engineering, University of Naples "Parthenope", 80143 Naples, Italy
[8]LSI, École Polytechnique, CEA/DRF/IRAMIS, CNRS, Institut Polytechnique de Paris, F-91128 Palaiseau, France
[9]Institute of Optical Sensor Systems, German Aerospace Center (DLR), 12489 Berlin, Germany
[10]Institute of Optics and Atomic Physics, TU Berlin, 10623 Berlin, Germany
[11]Department of Molecular Sciences and Nanosystems, Ca' Foscari University of Venice, 30172 Venezia-Mestre, Italy

Abstract

The understanding of how spins move and can be manipulated at pico- and femtosecond time scales is the goal of much of modern research in condensed matter physics, with implications for ultrafast and more energy-efficient data processing and storage applications. However, the limited comprehension of the physics behind this phenomenon has hampered the possibility of realising a commercial technology based on it. Recently, it has been suggested that inertial effects should be considered in the full description of the spin dynamics at these ultrafast time scales, but a clear observation of such effects in ferromagnets is still lacking. Here, we report the first direct experimental evidence of intrinsic inertial spin dynamics in ferromagnetic thin films in the form of a nutation of the magnetisation at a frequency of approximately 0.5 THz. This allows us to reveal that the angular momentum relaxation time in ferromagnets is on the order of 10 ps.

The vast majority of digital information worldwide is stored in the form of tiny magnetic bits in thin film materials in the hard-disk drives installed in large-scale data-centres. The position of the north and south magnetic poles with respect to the thin film plane encodes the logical "ones" and "zeros", which are written using strongly localised, intense magnetic fields. The dynamics of the magnetisation in the writing process is described by the Landau-Lifshitz-Gilbert (LLG) equation, which correctly models the reversal of a magnetic bit at nanosecond time-scales. Until 20 years ago, it was believed that all of the relevant physics of magnetisation dynamics was included in this equation and that optimisation of storage devices could be based solely on it.

However, the pioneering experiment of Bigot *et al.* in 1996 [1] revealed the occurrence of spin dynamics on the sub-picosecond scales that could not be described by the LLG equation, giving birth to the field of ultrafast magnetism. This field explores some of the currently most investigated and debated topics in condensed matter physics [2, 3, 4, 5, 6, 7, 8, 9, 10, 11, 12, 13, 14, 15, 16, 17, 18, 19, 20], with implications for both our fundamental understanding of magnetism as well as possible applications for faster and more energy-efficient data manipulation [21]. Recently, the LLG equation was reformulated including a term to obtain a physically correct inertial response, which was surprisingly missing from the original formulation [22, 23, 24, 25, 26, 27,

*e-mail: stefano.bonetti@fysik.su.se

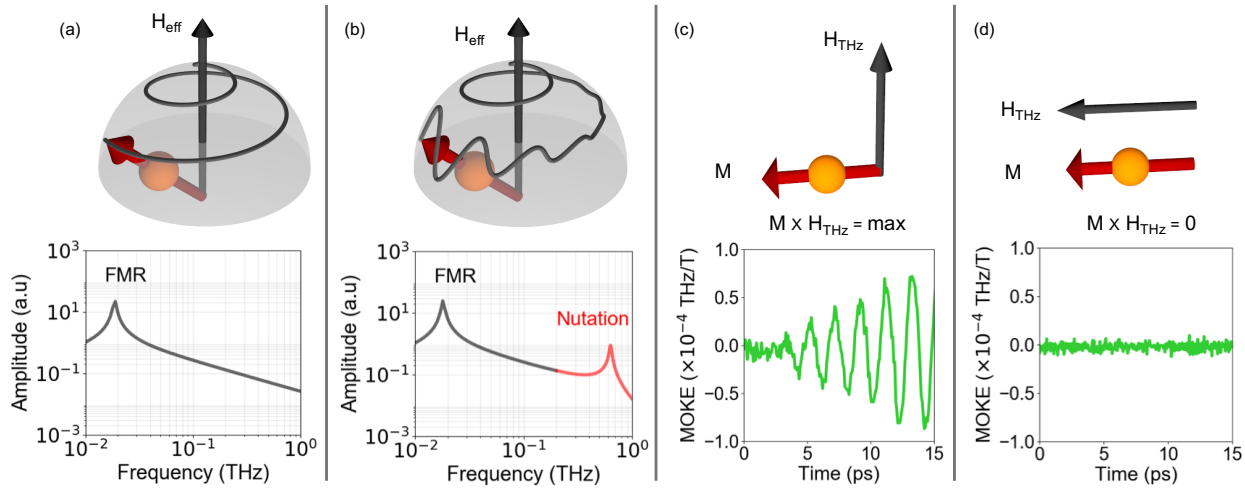

Figure 1: (a) Top panel: schematic of magnetisation dynamics and relaxation around an effective magnetic field H according to the standard LLG equation. Bottom panel: LLG-simulated response (i.e. the susceptibility) of a ferromagnetic system to an external ac magnetic field of varying frequency. (b) Similar to (a), but considering the inertial formulation of the LLG equation described in the text. (c) Top panel: the geometrical configuration which maximises the torque of $\mathbf{H}_{\mathrm{THz}}$ on the magnetisation $\mathbf{M}$, i.e. when they are orthogonal. Bottom panel: measured response from the polycrystalline NiFe sample in the maximum torque configuration and with a driving field centered at around 0.6 THz. (d) Similar to (c) but when $\mathbf{H}_{\mathrm{THz}}$ and $\mathbf{M}$ are parallel, no torque is exerted on the same sample by the same driving field.

28, 29, 30, 31, 32]. This term predicts the appearance of spin nutations, similar to the ones of a spinning top, at a frequency much higher (in the terahertz range) than the spin precession described by the conventional LLG equation, typically at gigahertz frequencies. However, the lack of intense magnetic field sources at these high frequencies has hampered the experimental observation of such nutation dynamics.

In this work, we use intense narrow-band terahertz magnetic field transients from a superradiant terahertz source and the femtosecond magneto-optical Kerr effect (MOKE), to detect inertial magnetisation effects in ferromagnetic thin films. We find evidence for nutation dynamics with a characteristic frequency of the order of 1 THz, which is damped on time scales of the order of 10 ps. We are able to qualitatively describe the observed magnetisation dynamics with a macrospin approximation of the inertial LLG equation and highlight implications for ultrafast magnetism, and magnetic data processing and storage.

According to the LLG equation, the dynamics of the magnetisation $\mathbf{M}$ in a ferromagnetic sample are described as [33]

$$\frac{d\mathbf{M}}{dt} = -|\gamma|\mathbf{M} \times \left(\mathbf{H}_{\mathrm{eff}} - \frac{\alpha}{|\gamma| M_s} \frac{d\mathbf{M}}{dt} \right), \tag{1}$$

where $|\gamma|/2\pi \approx 28$ GHz/T is the gyromagnetic ratio, $\mathbf{H}_{\mathrm{eff}}$ is the effective magnetic field, calculated as the variational derivative of energy with respect to the magnetisation, M_s is the saturation magnetisation, and α is the so-called Gilbert damping. The first term on the right-hand side describes the precession $\mathbf{M}$ of a ferromagnetic system around $\mathbf{H}_{\mathrm{eff}}$, while the second term is the damping term, which relaxes the system to an equilibrium state where $\mathbf{M}$ and $\mathbf{H}_{\mathrm{eff}}$ are parallel and no torque is exerted on the magnetisation. Fig. 1(a) illustrates schematically the magnetisation precession around the effective magnetic field. A resonance peak of the precession can be seen in the frequency domain and it corresponds to the so-called ferromagnetic resonance (FMR). Here, the motion of the spin system is treated as analogous to a classical spinning top. Hence, one can derive the equation of motion of spins in a magnetic field similar to that of a spinning top in a gravitational field. On a similar line, Gilbert introduced a Lagrangian for the ferromagnetic systems with an *ad hoc* inertia tensor. In this mechanical approach for describing the motion of spins the two principle moments of inertia were set to zero, so that the inertial terms disappear from the dynamic equation. But an inertial tensor of such kind is not physically correct as the same Gilbert noticed [33]. Despite its crudeness, this approximation turned out to be good enough to describe the dynamics of magnetisation on time scales of 0.1 nanoseconds or longer, and the general validity of the equation at faster time scales was not questioned.

The concept of mass and inertia in macroscopic systems (domain walls) was for the first time introduced by Döring [34] already in 1948. In 2004 Zhu *et al.* [35] showed that the dynamics of spins in a tunnelling barrier between two superconductors has an unusual spin behaviour in contrast to a simple spin precession and they termed it as "Josephson nutation". Kimel *et al.* [36] for the first time showed inertia-driven spin switching in antiferromagnetically ordered systems. According to Ref. [36], a very short (femtosecond) magnetic impulse

can impart enough energy to the spin system, so to overcome the potential barrier and flip its orientation. In the examples mentioned previously, the inertial terms are due to the non-homogeneity of the magnetic configurations (domain walls, antiferromagnetism, ferrimagnetism, etc), i.e. they are due to the presence of the exchange interaction between spins. However, the concept of intrinsic inertia for homogeneous magnetic configurations (typically for a single magnetic dipole or a single spin) arrived only later [22, 24, 25, 26, 27, 28, 29, 30, 31], and led to the so-called inertial LLG equation

$$\frac{d\mathbf{M}}{dt} = -|\gamma|\mathbf{M} \times \left[\mathbf{H}_{\text{eff}} - \frac{\alpha}{|\gamma|M_s}\left(\frac{d\mathbf{M}}{dt} + \tau\frac{d^2\mathbf{M}}{dt^2}\right)\right]. \tag{2}$$

The last term of Eq. (2) has a second derivative term (due to angular momentum relaxation), apart from the spin precession and damping. This term comes into the picture if one considers the moment of inertia while solving the Landau-Lifshitz (LL) equation based on the classical analogue of a spinning top [22, 37]. Simulations reveal that, on time scales shorter than τ, nutation oscillations are present on top of the precession motion, as shown in Fig. 1(b), identifying a novel "nutation regime" driven by intrinsic inertia that has yet to be observed experimentally. On time scales longer than τ the usual LLG equation is recovered. The possible large separation between the time scales of the two regimes would then explain the success of the standard LLG equation in correctly describing magnetisation dynamics for times larger than τ. The determination of the value of τ is, however, an open problem which needs to be addressed experimentally, as different theoretical studies indicate values ranging from a few femtoseconds to hundreds of picoseconds [22, 30, 32, 34, 37].

In order to attack this problem, one needs to be able to perform magnetic field spectroscopy in the terahertz range, a task which was technically unfeasible until very recently, when intense terahertz sources have started to become available. In the past few years, broadband terahertz radiation generated with table-top laser sources [38] has been exploited to study magnetisation dynamics in different classes of materials [39, 40, 41, 42, 43, 44]. In addition to demagnetisation effects similar to those observed with near-infrared radiation, the terahertz magnetic field $\mathbf{H}_{\text{THz}}$ of such intense radiation can exert a Zeeman torque $\mathbf{M} \times \mathbf{H}_{\text{THz}}$, leading to a coherent precessional motion of the magnetisation vector $\mathbf{M}$, which lasts until the THz pulse has left the material. Those table-top sources, while having the necessary terahertz bandwidth to perform the proposed magnetic field spectroscopy, are not spectrally dense, and the detection of a nutation resonance driven by inertia has not been reported yet.

However, intense and tunable narrow-band terahertz magnetic fields can now be generated at superradiant electron sources such as the TELBE facility in Dresden, Germany [45, 46]. Here, we used the radiation generated at TELBE to drive the magnetisation of thin film ferromagnets with a strong periodic terahertz magnetic field. The basic idea is to perform a forced oscillator experiment as a function of the frequency of the terahertz magnetic field $\mathbf{H}_{\text{THz}}$, detecting amplitude and phase of the response with the femtosecond MOKE, in the attempt to observe the signature of a resonance. The response of the magnetisation is maximised when $\mathbf{H}_{\text{THz}}$ and the static magnetisation (which is controlled with an external magnetic field) are orthogonal to each other. This is illustrated schematically in the top panels of Fig. 1(c) and 1(d), with the corresponding experimental measurement in the bottom panels, where we show the detected polar MOKE signal. That the terahertz-driven dynamics in thin magnetic films is a genuine magnetic effect and not an optical artefact has now been shown in several works. In Ref. [47] it is shown that the response of a similar magnetic film, when either the externally applied magnetic field or the terahertz magnetic field polarity are reversed, has the symmetry expected of a magnetic effect. The polar MOKE configuration is the optimal geometry since the torque acts out of the film plane when both $\mathbf{H}_{\text{THz}}$ and $\mathbf{M}$ are in the plane. Further details of the experimental setup are given in the Methods section. However, we comment here on the normalisation procedure, which is a key aspect when measuring absolute amplitudes. With the realistic assumptions that the first term on the right-hand side of Eq. (1) and Eq. (2) is much larger than the other terms, and that the magnetisation responds linearly to the field, one can read the response of the magnetisation as the integral of the terahertz magnetic field. Approximating the terahertz magnetic field as a sinusoidal excitation with angular frequency ω, in the case of orthogonal $\mathbf{M}$ and $\mathbf{H}_{\text{THz}}$, the temporal response of the normalised magnetisation $m(t) = M(t)/M_s$ ignoring resonance effects can be simplified as

$$m(t) = |\gamma| \int H_{\text{THz}} \sin\omega t \, dt = |\gamma| \frac{H_{\text{THz}}}{\omega} \cos\omega t, \tag{3}$$

with the magnetisation starting to move out of the plane of the film when $\mathbf{M}$ and $\mathbf{H}$ are in the film plane. Hence, in order to estimate the proper response of the magnetic films to the terahertz magnetic field, the data presented in Fig. 2 and Fig. 4 has been normalised by the magnitude H_{THz} and by the frequency ω of the THz pulse.

We investigated three different thin film samples, all with easy-plane magnetisation: amorphous CoFeB grown on a Si/SiO_2 substrate, whereas epitaxial and polycrystalline permalloy films were grown on single crystal MgO (100) and (111) substrates respectively. Those samples have different Gilbert damping parameter

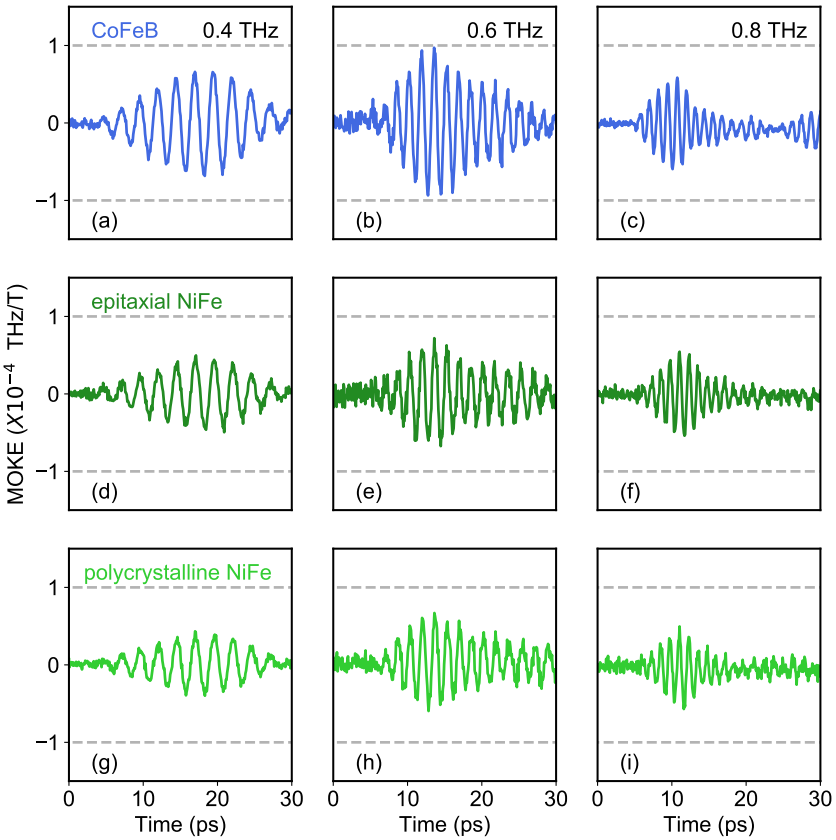

Figure 2: Time-resolved magneto-optical Kerr (MOKE) response of the magnetisation to narrowband terahertz fields centered around 0.4, 0.6 and 0.8 THz for (a)-(c) an amorphous CoFeB film on silicon, (d)-(f) an epitaxial $Ni_{81}Fe_{19}$ (permalloy) film grown on MgO (100) substrate and (g)-(i) of a polycrystalline $Ni_{81}Fe_{19}$ deposited on MgO (111) substrate. The data is normalised according to Eq. (3) and related considerations in the main text.

α, and saturation magnetisation M_s. Both parameters modulate the magnitude of the additional inertial term introduced in Eq. (2).

Figure 2 shows the amplitude of the femtosecond MOKE response of the three ferromagnetic thin film samples after excitation with narrowband terahertz pulses with a centre frequency of 0.4, 0.6 and 0.8 THz. The characterisation of the narrowband terahertz pulses, performed with electro-optical sampling, is described in the Methods section. The terahertz magnetic field was applied orthogonal to the equilibrium magnetisation direction as discussed above, so to maximise the torque. In all cases, a clear coherent response of the magnetisation to the narrowband terahertz field is observed. After the normalisation procedure discussed above, the overall response seems to be slightly larger for the CoFeB samples, likely related to the larger magneto-optical response of that sample as compared to permalloy. Hence, to infer real magnetic effects (as compared to magneto-optical ones), absolute amplitudes should be compared only within the same sample at different frequencies, and not between different samples. With this consideration, one can observe an evident change in the amplitude of the response within each sample when the frequency is changed, with the largest effect observed at approximately 0.5-0.6 THz for all three cases.

The observed response of the magnetisation confirms the analogy with a forced oscillator, where the terahertz magnetic field acts as the driving periodic force, to which the magnetisation responds, in the linear regime, by integrating it. The modulation of the amplitude of the response suggests already the presence of an underlying resonance at approximately 0.6 THz superimposed to the purely off-resonant, forced response of lower amplitude. To further validate this point, in Fig. 3 we analysed the relative phase shift between the integral of the driving force (the terahertz magnetic field, which is reconstructed independently via experimental electro-optical sampling) and the experimental MOKE signal far away from the maximum response (0.4 THz) and close to the maximum response (0.6 THz). We show here data for one of the samples, but similar trends are observed for the other two (see Supplementary Information). The data shows that at 0.4 THz the magnetisation precession is in phase with the driving field, and this is also reproduced by simulations solving the inertial LLG equation [25, 48] including the experimentally measured terahertz magnetic field as the driving force. (See Methods section for details.) At 0.6 THz, on the other hand, magnetisation precession and driving field are approximately 90 degrees out of phase, which is also reproduced by the simulations. This fact reinforces the statement that an underlying resonance is present in the system, at a frequency two orders of magnitude higher

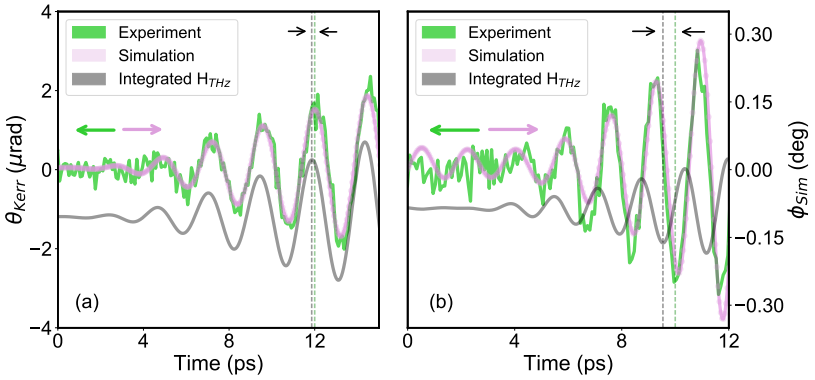

Figure 3: Comparison of the phase resolved response at (a) 0.4 THz and (b) 0.6 THz center frequency of the terahertz magnetic field pulse for the polycrystalline permalloy film. Green curves: experimentally measured magneto-optical Kerr rotations, without the scaling described by Eq. (3). The absolute value of rotation for both frequencies are plotted on the left vertical axis. Pink curves: simulated response using the inertial LLG equation with $\tau = 11.3$ ps and using the experimentally measured H_{THz} field amplitude. The right vertical axis is the simulated nutation angle. Grey curves: time integral of the experimental terahertz magnetic field H_{THz}.

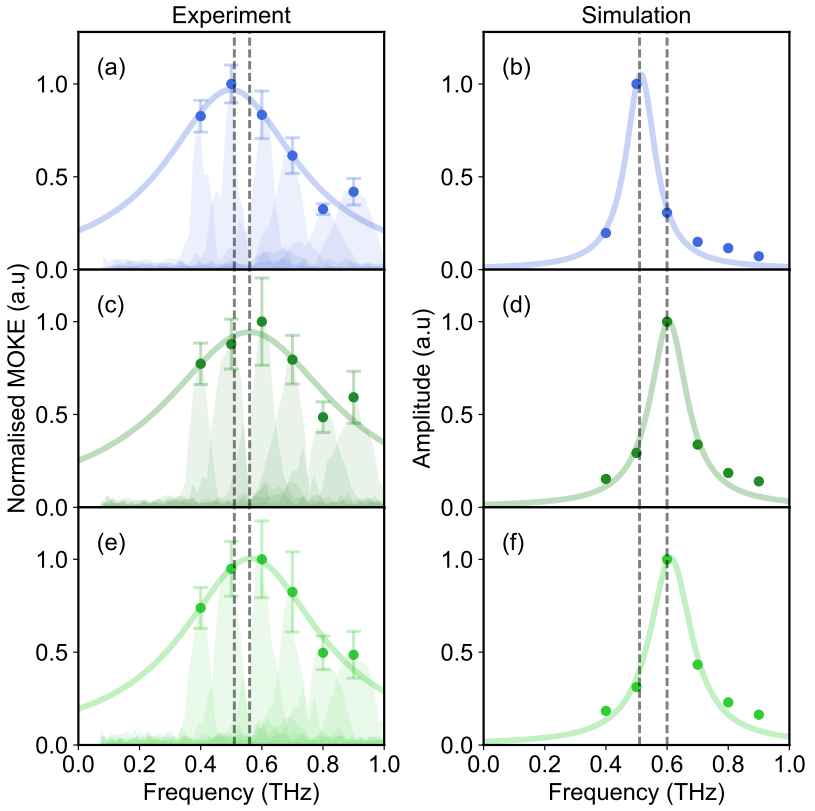

Figure 4: Symbols: (a), (c), (e) experimentally measured maximum of the MOKE amplitude normalized according to Eq. (3) for CoFeB, epitaxial NiFe and, respectively, polycrystalline NiFe. The shaded curves represent the magnitude of the Fourier transform of the experimental traces at the different center frequencies. Error bars represent the standard deviation of noise before the arrival of the terahertz pulse, first measured in absolute units and then scaled by the same amplitude with the signal. (b), (d), (f) calculated maximum magnetisation response amplitude solving the inertial LLG equation. Solid lines: Lorentzian fit to the data points.

than any known ferromagnetic resonance, and which is determined by one single fitting parameter τ, i.e. the angular momentum relaxation term in Eq. (2).

In order to estimate the value of τ from experiments, we plot in Fig. 4(a) the amplitude of the measured response at six different frequencies. A fit with a Lorentzian curve was used to return the centre frequency ω_n.

Sample	Center frequency $\omega_n/2\pi$ (THz)	FWHM (THz)	α	$\tau = 1/\alpha\omega_n$ (ps)
CoFeB	0.50 ± 0.10	0.58	0.0044	$72\,[-13, +17]$
epitaxial NiFe	0.56 ± 0.12	0.67	0.0058	$49\,[-\ 9, +13]$
polycrystalline NiFe	0.56 ± 0.11	0.55	0.0230	$12\,[-\ 2, +\ 3]$

Table 1: The center frequency ω_n and the full-width half maximum (FWHM) were extracted parameters from the Lorentzian fit of the experimental data plotted in Fig. 4 for all three samples. The Gilbert damping α was measured independently. The angular momentum relaxation time τ is calculated using the approximation of Eq.(4).

According to Ref. [27], the nutation frequency is

$$\omega_n = \frac{\sqrt{1 + \alpha\tau|\gamma|H}}{\alpha|\gamma|} \approx 1/\alpha\tau. \tag{4}$$

We measured the Gilbert damping α independently with ferromagnetic resonance spectroscopy in all three samples and extracted the corresponding τ, as summarised in Table 1. Numerical calculations that solve the inertial LLG equation with these values of τ are shown in Fig. 4(b), and reproduce the main features of the experimental data.

We now make several considerations looking at Fig. 4 and Table 1. The first observation is that the peak centre frequency moves by approximately 10% between the different materials, almost independently of α. Interestingly, even though the relative uncertainty is large, the nutation frequency for the two NiFe samples is the same, and slightly different from the one of the CoFeB sample. The nutation frequency ω_n is also very weakly dependent on the applied magnetic field; solving the inertial LLG equation, we estimated that one would need a 10 T applied field to shift the peak by approximately 200 GHz, which should be detectable even given the large width of the resonance. The measured nutation frequencies are, for all samples, in the range predicted by Ref. [32].

A second important observation is that the width of the experimental peak is larger than what simulations predict. This mismatch can potentially be attributed to the fact that the inertial motion of the spins might be affected by the microscopic details of the material. The inertial dynamics has been reported to remain the same if one considers the dynamics of a macroscopic magnetic volume element [29]. However, it is surprising that the different materials with different textures that we investigate here, show no appreciable difference in linewidth. We have performed micromagnetic simulations and did not observe substantial linewidth broadening. We have also checked that finite temperature effects, included in the simulations as a random fluctuation of the effective magnetic field acting on the magnetisation, did not substantially affect the linewidth. Further considerations are beyond the scope of this work and we leave this question open to future investigations.

Finally, we comment on the experimentally extracted values of τ of the order of 10-100 ps. These are one to two orders of magnitude larger than the ones obtained with indirect spectroscopy experiments observing the stiffening of the ferromagnetic resonance, but with no phase information [48]. This is a discrepancy that we cannot reconcile at the moment, but we believe that our direct measurement of the resonant nutation frequency, with amplitude and phase information, gives a more accurate estimate of the relaxation time. The extracted τ is also greater than the one observed in recent studies looking at the relaxation of the magnetisation with phonons [17, 19] and magnons [12, 18, 20]. However, in all these cases, an essential ingredient was the excitation of hot electrons $\sim$ 1 eV away from the Fermi level by means of femtosecond near-infrared radiation. In this work, the much lower photon energy ($\sim$ 1 meV) of the driving terahertz field prevents by design the creation of such hot electrons. Hence, a direct comparison between the relaxation time scale of our experiment and the one observed in these studies cannot be made.

An alternative explanation for the presence of a high-frequency magnetic excitation could be the presence of exchange-dominated standing spin-wave modes across the film thickness, similar to what was observed in Ref. [49]. However, we argue that those modes are not relevant here, simply because they cannot be excited in our experiment. In fact, we directly drive the film with electromagnetic radiation whose k-vector is orders of magnitude smaller than the film thickness, and far away from such high-k spin waves. Excitation of large wave-number spin waves due to ultrafast demagnetisation, caused by the terahertz-induced spin currents observed in Ref. [41], are also not expected. In metals and at terahertz frequencies, the skin depth is of the order of 0.1 - 1 μm, again orders of magnitude larger than the thin film thickness, hence any spin current related effects are, to an excellent approximation, uniform in the sample. At present, our data clearly demonstrate the existence of a resonance in the terahertz regime, whose most plausible theoretical explanation is the excitation of intrinsic nutation dynamics in the magnetic system.

In conclusion, we used narrowband terahertz magnetic fields to drive magnetisation dynamics in thin ferromagnetic films, which we probed with the femtosecond magneto-optical Kerr effect. By analysing both amplitude and phase of the response, we detect the appearance of a broad resonance at approximately 0.5 THz, which we ascribe to the presence of a nutation spin resonance excited by the terahertz magnetic field. Our experimental

observations are in good agreement with numerical simulations performed with the intrinsic inertial version of the LLG equation using the angular momentum relaxation time τ extracted from the experimental data. We anticipate that our results will allow for a better understanding of the fundamental mechanisms of ultrafast demagnetisation and reversal, with implications for the realisation of faster and more efficient magnetic data processing and storage devices.

Acknowledgements

We thank Jürgen Lindner (HZDR, Dresden) for helpful discussion. The research leading to this result has been supported by the project CALIPSOplus under Grant Agreement 730872 from the EU Framework Programme for Research and Innovation HORIZON 2020. Parts of this research were carried out at ELBE at Helmholtz-Zentrum Dresden-Rossendorf e.V., a member of the Helmholtz Association. We would like to thank Ulf Lehnert and Jochen Teichert for assistance, and the ELBE team for operating the TELBE facility. S.K., B.G., and M.G. acknowledge support from the European Cluster of Advanced Laser Light Sources (EUCALL) project, which has received funding from the European Union's Horizon 2020 research and innovation programme under Grant Agreement No 654220. N.A., I.I., M.G. and S.K. acknowledge support from the European Commission's Horizon 2020 research and innovation programme, under Grant Agreement No DLV-737038(TRANSPIRE). K.N., D.P., N.Z.H. and S.B. acknowledge support from the European Research Council, Starting Grant 715452 MAGNETIC-SPEED-LIMIT.

Author Contributions

S.B. designed the experiment, S.B. and M.G. coordinated the project; K.N., N.A., S.K., D.P., N.Z.H., B.G., J.C.D., I.I., M.C., M.B., M.G. and S.B. performed the measurements at TELBE; K.N., N.A. and S.B. performed the data analysis; K.N., V.S., M.d'A. and C.S. performed the inertial LLG simulations. S.S.P.K.A., O.H, A.S., K.L. fabricated and characterised the samples; K.N. and S.B. coordinated the work on the paper with contributions from N.A., S.K., S.S.P.K.A., A.S., K.L., O.H., J.E.W., M.G. and discussions with all authors.

Corresponding authors

Correspondence to S. Bonetti.

Methods

Sample details

The epitaxial permalloy ($Ni_{81}Fe_{19}$ at. %) films investigated in the study are 15 nm thick and prepared by magnetron sputter deposition using Ar sputter gas at $P_{Ar} = 3.5 \times 10^{-3}$ mbar. At first, single crystal MgO (100) substrates were pre-annealed at 873 K for 3 hours to remove typical inorganic Mg(OH) layers from the surface, then the substrate was cooled down to 550 K for DC - magnetron sputtering. The epitaxial relation between the substrate and the films ($MgO(100)[100]_{fcc}||Ni_{81}Fe_{19}(100)[100]_{fcc}$, c/a ratio of 0.99) were confirmed by XRD (ϕ-scans along (111) orientation of the MgO crystal and the NiFe film). After the same substrate pre-annealing step as used above (873 K for 3 hours), 15 nm thick polycrystalline $Ni_{81}Fe_{19}$ films were deposited at room temperature on a MgO (111) substrate. In both cases (epitaxial and polycrystalline Py), an Al cap layer of 1.5 nm was deposited at room temperature to protect the magnetic films from oxidation. The atomic stoichiometry of the $Ni_{81}Fe_{19}$ alloy thin-films were determined by Rutherford Backscattering Spectrometry (RBS) within the measurement accuracy of ± 1 at.%.

Amorphous 10 nm thick $Co_{40}Fe_{40}B_{20}$ films were sputter-deposited at room temperature from a stoichiometric target on a Si/SiO_2(100 nm)/Al_2O_3(10 nm) substrate, followed by an Al (1.5 nm) cap layer. Commercial 2-inch stoichiometric alloy targets of $Ni_{81}Fe_{19}$, $Co_{40}Fe_{40}B_{20}$, (4N material purity) were produced by liquid metallurgy. The deposition rates were pre-calibrated using X-ray reflectivity measurements (XRR) and during the sputtering process, the thicknesses of the individual layers were monitored via a quartz crystal. The saturation magnetisation M_s was determined from 3 mm $\times$ 3 mm sample pieces using SQUID-VSM, and we found the values $M_s = 756$ kA/m ($\mu_0 M_s = 0.95$ T) for epitaxial permalloy, $M_s = 738$ kA/m ($\mu_0 M_s = 0.93$ T) for polycrystalline permalloy, and $M_s = 1290$ kA/m ($\mu_0 M_s = 1.62$ T) for amorphous CoFeB.

Experimental setup

The superradiant THz pulse source TELBE delivered multicycle electromagnetic pulses at a repetition rate of 100 kHz. The generated THz pulses are linearly polarized with a spectral bandwidth of 20%, and with a center frequency tunable between 0.3 and 1.2 THz [46]. In the experiment described here, the THz radiation from TELBE was focused onto the sample using gold-coated off-axis parabolic mirrors. The THz electric field was measured in the time-domain by free-space electro-optical sampling in a 100 μm thick ZnTe crystal. A 100 fs duration laser pulse with a central wavelength of 805 nm, from a commercial Ti:sapphire laser system is used as a probe. The laser is synchronised with the TELBE source, with a typical timing jitter of approximately 30 fs (FWHM) between the probe laser and the THz pulse generated from the undulator [46, 50].

In our measurement scheme, the samples were magnetised in plane using an externally applied magnetic field of 0.35 T using a permanent magnet. The coherent response of the sample magnetisation to the THz field was probed by measurements of the magneto-optical Kerr effect (MOKE) in polar geometry (i.e. at normal incidence). Further details about the measurement geometry are given in the Supplementary Information. In our analysis, we define a time zero looking at the electro-optical sampling data just before the first detectable oscillation of the THz waveform. We then kept the same time zero (i.e. the same position of the delay stage) of all the MOKE scans for the respective frequency.

MOKE data normalization

The normalized MOKE curves in Fig. 2 obtained from the reflectivity data were calculated as:

$$MOKE = \frac{\Delta R}{2R} \times \frac{\omega/2\pi}{H_{\mathrm{THz}}}, \tag{5}$$

where ΔR is the transient reflectivity change due to the THz pump, ω is the center frequency of the terahertz pump field and H_{THz} its maximum amplitude. Error bars in the resonance amplitude are calculated by taking the standard deviation of the measurement before time zero.

References

1. Beaurepaire, E, Merle, J.-C., Daunois, A & Bigot, J.-Y. Ultrafast spin dynamics in ferromagnetic nickel. *Physical Review Letters* **76,** 4250 (1996).
2. Koopmans, B., Van Kampen, M, Kohlhepp, J. T. & De Jonge, W. J. M. Ultrafast magneto-optics in nickel: magnetism or optics? *Physical Review Letters* **85,** 844 (2000).
3. Koopmans, B, Van Kampen, M & De Jonge, W. Experimental access to femtosecond spin dynamics. *Journal of Physics: Condensed Matter* **15,** S723 (2003).
4. Koopmans, B., Ruigrok, J., Dalla Longa, F. & De Jonge, W. Unifying ultrafast magnetization dynamics. *Physical Review Letters* **95,** 267207 (2005).
5. Stamm, C *et al.* Femtosecond modification of electron localization and transfer of angular momentum in nickel. *Nature Materials* **6,** 740 (2007).
6. Dalla Longa, F, Kohlhepp, J., De Jonge, W. & Koopmans, B. Influence of photon angular momentum on ultrafast demagnetization in nickel. *Physical Review B* **75,** 224431 (2007).
7. Carpene, E. *et al.* Dynamics of electron-magnon interaction and ultrafast demagnetization in thin iron films. *Physical Review B* **78,** 174422 (2008).
8. Koopmans, B *et al.* Explaining the paradoxical diversity of ultrafast laser-induced demagnetization. *Nature Materials* **9,** 259 (2010).
9. Boeglin, C. *et al.* Distinguishing the ultrafast dynamics of spin and orbital moments in solids. *Nature* **465,** 458 (2010).
10. Kirilyuk, A., Kimel, A. V. & Rasing, T. Ultrafast optical manipulation of magnetic order. *Reviews of Modern Physics* **82,** 2731 (2010).
11. Battiato, M., Carva, K. & Oppeneer, P. M. Superdiffusive spin transport as a mechanism of ultrafast demagnetization. *Physical Review Letters* **105,** 027203 (2010).
12. Schmidt, A. *et al.* Ultrafast magnon generation in an Fe film on Cu (100). *Physical Review Letters* **105,** 197401 (2010).
13. Radu, I *et al.* Transient ferromagnetic-like state mediating ultrafast reversal of antiferromagnetically coupled spins. *Nature* **472,** 205 (2011).

14. Mathias, S. *et al.* Probing the timescale of the exchange interaction in a ferromagnetic alloy. *Proceedings of the National Academy of Sciences* **109,** 4792–4797 (2012).

15. Carva, K., Battiato, M., Legut, D. & Oppeneer, P. M. Ab initio theory of electron-phonon mediated ultrafast spin relaxation of laser-excited hot electrons in transition-metal ferromagnets. *Physical Review B* **87,** 184425 (2013).

16. Lambert, C.-H. *et al.* All-optical control of ferromagnetic thin films and nanostructures. *Science* **345,** 1337–1340 (2014).

17. Henighan, T *et al.* Generation mechanism of terahertz coherent acoustic phonons in Fe. *Physical Review B* **93,** 220301 (2016).

18. Eich, S. *et al.* Band structure evolution during the ultrafast ferromagnetic-paramagnetic phase transition in cobalt. *Science Advances* **3,** e1602094 (2017).

19. Dornes, C. *et al.* The ultrafast Einstein–de Haas effect. *Nature,* 1 (2019).

20. Iacocca, E. *et al.* Spin-current-mediated rapid magnon localisation and coalescence after ultrafast optical pumping of ferrimagnetic alloys. *Nature communications* **10,** 1–11 (2019).

21. Stanciu, C. *et al.* Subpicosecond magnetization reversal across ferrimagnetic compensation points. *Physical Review Letters* **99,** 217204 (2007).

22. Ciornei, M.-C., Rubí, J. & Wegrowe, J.-E. Magnetization dynamics in the inertial regime: Nutation predicted at short time scales. *Physical Review B* **83,** 020410 (2011).

23. Böttcher, D, Ernst, A & Henk, J. Atomistic magnetization dynamics in nanostructures based on first principles calculations: application to Co nanoislands on Cu (111). *Journal of Physics: Condensed Matter* **23,** 296003 (2011).

24. Wegrowe, J.-E. & Ciornei, M.-C. Magnetization dynamics, gyromagnetic relation, and inertial effects. *American Journal of Physics* **80,** 607–611 (2012).

25. Olive, E., Lansac, Y. & Wegrowe, J.-E. Beyond ferromagnetic resonance: The inertial regime of the magnetization. *Applied Physics Letters* **100,** 192407 (2012).

26. Bhattacharjee, S., Nordström, L. & Fransson, J. Atomistic spin dynamic method with both damping and moment of inertia effects included from first principles. *Physical Review Letters* **108,** 057204 (2012).

27. Olive, E., Lansac, Y., Meyer, M, Hayoun, M & Wegrowe, J.-E. Deviation from the Landau-Lifshitz-Gilbert equation in the inertial regime of the magnetization. *Journal of Applied Physics* **117,** 213904 (2015).

28. Thonig, D., Eriksson, O. & Pereiro, M. Magnetic moment of inertia within the torque-torque correlation model. *Scientific Reports* **7,** 931 (2017).

29. Mondal, R., Berritta, M. & Oppeneer, P. M. Generalisation of Gilbert damping and magnetic inertia parameter as a series of higher-order relativistic terms. *Journal of Physics: Condensed Matter* **30,** 265801 (2018).

30. Kikuchi, T. & Tatara, G. Spin dynamics with inertia in metallic ferromagnets. *Physical Review B* **92,** 184410 (2015).

31. Fähnle, M. Comparison of theories of fast and ultrafast magnetization dynamics. *Journal of Magnetism and Magnetic Materials* **469,** 28–29 (2019).

32. Bastardis, R., Vernay, F. & Kachkachi, H. Magnetization nutation induced by surface effects in nanomagnets. *Physical Review B* **98,** 165444 (2018).

33. Gilbert, T. L. A phenomenological theory of damping in ferromagnetic materials. *IEEE Transactions on Magnetics* **40,** 3443–3449 (2004).

34. Böttcher, D & Henk, J. Significance of nutation in magnetization dynamics of nanostructures. *Physical Review B* **86,** 020404 (2012).

35. Zhu, J.-X., Nussinov, Z., Shnirman, A. & Balatsky, A. V. Novel spin dynamics in a Josephson junction. *Physical Review Letters* **92,** 107001 (2004).

36. Kimel, A. *et al.* Inertia-driven spin switching in antiferromagnets. *Nature Physics* **5,** 727 (2009).

37. Fähnle, M., Steiauf, D. & Illg, C. Generalized Gilbert equation including inertial damping: Derivation from an extended breathing Fermi surface model. *Physical Review B* **84,** 172403 (2011).

38. Hoffmann, M. C. & Fülöp, J. A. Intense ultrashort terahertz pulses: generation and applications. *Journal of Physics D: Applied Physics* **44,** 083001 (2011).

39. Kampfrath, T., Tanaka, K. & Nelson, K. A. Resonant and nonresonant control over matter and light by intense terahertz transients. *Nature Photonics* **7,** 680 (2013).

40. Vicario, C. *et al.* Off-resonant magnetization dynamics phase-locked to an intense phase-stable terahertz transient. *Nature Photonics* **7,** 720 (2013).

41. Bonetti, S. *et al.* THz-driven ultrafast spin-lattice scattering in amorphous metallic ferromagnets. *Physical Review Letters* **117,** 087205 (2016).

42. Hafez, H. A. *et al.* Extremely efficient terahertz high-harmonic generation in graphene by hot Dirac fermions. *Nature* **561,** 507 (2018).

43. Noe, G. *et al. Coherent Terahertz Excitation of Magnons to 30 T* in *2018 Conference on Lasers and Electro-Optics (CLEO)* (2018), 1–2.

44. Polley, D. *et al.* THz-driven demagnetization with perpendicular magnetic anisotropy: towards ultrafast ballistic switching. *Journal of Physics D: Applied Physics* **51,** 084001 (2018).

45. Kovalev, S *et al.* Probing ultra-fast processes with high dynamic range at 4th-generation light sources: Arrival time and intensity binning at unprecedented repetition rates. *Structural Dynamics* **4,** 024301 (2017).

46. Kovalev, S *et al.* Selective THz control of magnetic order: new opportunities from superradiant undulator sources. *Journal of Physics D: Applied Physics* **51,** 114007 (2018).

47. Hudl, M. *et al.* Nonlinear magnetization dynamics driven by strong terahertz fields. *Physical review letters* **123,** 197204 (2019).

48. Li, Y., Barra, A.-L., Auffret, S., Ebels, U. & Bailey, W. E. Inertial terms to magnetization dynamics in ferromagnetic thin films. *Physical Review B* **92,** 140413 (2015).

49. Razdolski, I. *et al.* Nanoscale interface confinement of ultrafast spin transfer torque driving non-uniform spin dynamics. *Nature Communications* **8,** 15007 (2017).

50. Green, B *et al.* High-field high-repetition-rate sources for the coherent THz control of matter. *Scientific Reports* **6,** 22256 (2016).